

# Gaseous SO<sub>3</sub> and H<sub>2</sub>SO<sub>4</sub> in the exhaust of an aircraft gas turbine engine: measurements by CIMS and implications for fuel sulfur conversion to sulfur (VI) and conversion of SO<sub>3</sub> to H<sub>2</sub>SO<sub>4</sub>

A. Sorokin<sup>a,\*</sup>, E. Katragkou<sup>a</sup>, F. Arnold<sup>a</sup>, R. Busen<sup>b</sup>, U. Schumann<sup>b</sup>

<sup>a</sup> Atmospheric Physics Division, Max Planck Institute for Nuclear Physics, P.O. Box 103980, Heidelberg 69029, Germany

<sup>b</sup> DLR Oberpfaffenhofen, Institute für Physik der Atmosphäre, Weßling, Germany

Received 7 May 2003; received in revised form 12 September 2003; accepted 29 September 2003

## Abstract

An estimation of the conversion efficiency ( $\varepsilon$ ) of fuel sulfur to SO<sub>3</sub> and H<sub>2</sub>SO<sub>4</sub>, where  $\varepsilon = ([\text{SO}_3] + [\text{H}_2\text{SO}_4])/[\text{S}_T]$  and  $[\text{S}_T]$  is the total sulfur atom concentration in the exhaust at the exit of an aircraft gas-turbine combustor, was derived from measurements by comparison with model results. The major results of the presented CIMS experiments and their interpretation with a model simulation are: (i) The efficiency is  $\varepsilon = 2.3 \pm 1\%$  at an exhaust age of about 5 ms from the combustor exit; (ii) The SO<sub>3</sub> molecules represent a major fraction of sulfur (VI) gases  $\varepsilon_A < 50\%$  and an essential SO<sub>3</sub>-conversion to H<sub>2</sub>SO<sub>4</sub> takes place in the sampling line where the exhaust gases spend a sufficiently long time and where the temperature is lower than in the hot exhaust. The coincidence of  $\varepsilon$  from our work (measurements with the sampling point in the exhaust just behind the combustor exit) and  $\varepsilon$  the measurements in an exhaust at a plume age of about 1 s suggests that the sulfur (VI) formation is inefficient in the post-combustor flow inside the aircraft engine.

© 2003 Elsevier Ltd. All rights reserved.

**Keywords:** Chemiions; Combustion; Ion clusters; Fuel sulfur conversion

## 1. Introduction

Gaseous sulfuric acid formed in aircraft engines (Frenzel and Arnold, 1994; IPCC, 1999) is of considerable current interest as it plays a potentially important role in forming and activating aerosol particles which become water vapor condensation nuclei (Zhao and Turco, 1995; Karcher, 1996). The latter promote the formation of contrails and potentially even of clouds. Gaseous H<sub>2</sub>SO<sub>4</sub> is formed via fuel sulfur oxidation to SO<sub>3</sub>, which in the cooling exhaust rapidly reacts with

water vapor leading to H<sub>2</sub>SO<sub>4</sub> (Reiner and Arnold, 1993). In the cooling exhaust GSA becomes supersaturated and condenses along with some water vapor on pre-existing soot particles leading to a partial H<sub>2</sub>SO<sub>4</sub>/H<sub>2</sub>O coating of soot particles (Zhao and Turco, 1995; Karcher, 1998). The H<sub>2</sub>SO<sub>4</sub>/H<sub>2</sub>O coating increases the hygroscopicity of a soot particle, thereby allowing the coated soot particle to act as a water vapor condensation nucleus at a lower water vapor supersaturation than the particles without coating. Furthermore, H<sub>2</sub>SO<sub>4</sub> may also experience homogeneous and/or heterogeneous ion-induced nucleation (Yu and Turco, 1997) leading to new volatile aerosol particles which grow by H<sub>2</sub>SO<sub>4</sub>/H<sub>2</sub>O condensation.

Soot coating and new particle formation and growth become more efficient as the GSA production  $P_{\text{GSA}}$  (i.e. mass of H<sub>2</sub>SO<sub>4</sub> produced per second) increases. The

\*Corresponding author. Fax: +49-6221-516324.

E-mail address: andrey.sorokin@mpi-hd.mpg.de

(A. Sorokin).

<sup>1</sup>Permanent address: Central Institute of Aviation Motors, Aviamotornaya 2, 111116, Moscow, Russia (sorokin@ciam.ru).

latter is  $P_{\text{GSA}} = \text{FF FSC } \varepsilon W_{\text{A}}/W_{\text{S}}$ . Here FF is the fuel flow into the engine combustor (kg/s), FSC is the fuel-sulfur content (kg of sulfur per kg of fuel),  $\varepsilon$  is the efficiency of fuel-sulfur conversion to  $\text{SO}_3$  and  $\text{H}_2\text{SO}_4$  that is equal to a ratio of concentrations ( $[\text{SO}_3] + [\text{H}_2\text{SO}_4]/[\text{S}_{\text{T}}]$ ), where  $[\text{S}_{\text{T}}]$  is the total concentration of sulfur atoms in the exhaust and finally  $W_{\text{A}}$  and  $W_{\text{S}}$  are the molecular weight of  $\text{H}_2\text{SO}_4$  and S, respectively. While FF is well known and FSC can be easily determined, the quantity  $\varepsilon$  is not yet well known. Previously reported  $\varepsilon$  values range between 0.005 and 0.7 (IPCC, 1999; Schumann et al., 2002). Theoretical model calculations yielded  $\varepsilon$  mostly between 0.005 and 0.1 (Schumann et al., 2002). Thus there is a very unsatisfactory situation regarding the critical importance of  $\varepsilon$  for fuel sulfur induced formation of volatile particles, contrails, and cirrus clouds.

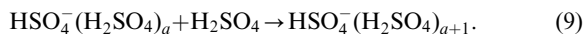
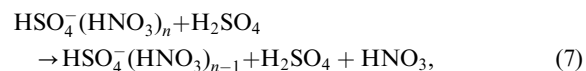
Gaseous  $\text{H}_2\text{SO}_4$  formation is thought to proceed via  $\text{SO}_2$  oxidation to  $\text{SO}_3$  and then to  $\text{H}_2\text{SO}_4$ . Sulfuric acid and its precursor  $\text{SO}_3$  have been measured previously by MPI-K, Heidelberg in jet aircraft engine exhaust at the ground. These measurements yielded  $\varepsilon$  ranging between 1% and 2% (Curtius et al., 1998) and  $2 \pm 0.8\%$  (Kieudler and Arnold, 2002a). Moreover, the group has measured the total  $\text{H}_2\text{SO}_4$  content (in gaseous and aerosol phases) in the plume of a jet aircraft in flight. These measurements yielded  $\varepsilon = 3.3 \pm 1.8\%$  (Curtius et al., 2002). The most important questions are: (i) which fraction of sulfur (VI) gases present in the aircraft engine exhaust is formed already in the combustor and (ii) which fraction of sulfur (VI) is emitted as  $\text{SO}_3$  molecules? The first gaseous S(VI) measurements performed at the exit of an aircraft engine yielded conversion efficiencies  $\varepsilon$  ranging between  $0.9 \pm 0.5\%$  and  $2.3 \pm 1.2\%$  depending on combustor operating conditions (Katragkou et al., 2003). The present paper reports on measurements at ground level of gaseous sulfuric acid,  $\text{SO}_3$ , and  $\varepsilon$  in the exhaust of an aircraft jet engine burning fuel with  $\text{FSC} = 212$  ppm and their interpretation using model calculations.

## 2. Experimental

The measurements to be reported here were made during the SULFUR campaign in the same aircraft jet engine exhaust and by the same flow-tube mass spectrometer apparatus as the chemiion measurements described by Arnold et al. (1998). However, for the present chemical ionization mass spectrometry (CIMS) measurements of gaseous sulfuric acid (GSA) and  $\text{SO}_3$  an additional capillary ion source (CIS) was used. From the external CIS reagent ions of the type  $\text{NO}_3^-(\text{HNO}_3)_a$  ( $a = 0, 1, 2$ ) were introduced into the flow tube (FT) via a capillary. Exhaust gas was sampled by an orifice probe (OP; diameter 0.3 cm) located at the front end of the FT

and directly at the plume axis at a distance of  $d = 1$  m downstream of the exit plane of the jet engine (Type RR M45 H). After entering the FT, exhaust gas was sucked through the FT (inner diameter: 4 cm; length 4.3 m) by a mechanical pump which was attached to the rear end of the FT. The total gas pressure in the FT was  $P_{\text{FT}} = 30$  hPa and the time span for gas passage through the FT was  $t_{\text{FT}} = 150$  ms. The point of reagent-ion introduction into the FT was located at a distance of 300 cm downstream of the OP. Thus the time for ions to react with trace gases was  $t_{\text{react}} = 45\text{--}50$  ms.

Upon introduction the reagent ions may react with GSA and  $\text{SO}_3$  via the ion molecule ligand and/or charge-transfer reactions the main of which are the following:



The measured rate coefficients of such reactions are very close to the expected ion-molecule collision rate coefficients of  $\sim 10^{-9}$  cm<sup>3</sup>/s (Su and Chesnavich, 1982; Arnold et al., 1998). Hydrated ion clusters may also be involved in ion-molecule reactions with sulfur-bearing neutral molecules (Arnold et al., 1995; Viggiano et al., 1997). After  $t_{\text{FT}} = 150$  ms the ions arrive at the rear end of the FT where a small fraction of the ions and gases enter the mass spectrometer vacuum chamber via a small entrance orifice (diameter: 0.02 cm). The chamber was pumped by a pump unit consisting of a backing pump and a cryogenic pump.

At the sampling point in a free exhaust plume the total sulfur concentration  $[\text{S}_{\text{T}}]_{\text{P}}$  was  $5 \times 10^{13}$  cm<sup>-3</sup>. This was determined from the measured  $\text{CO}_2$  concentration, the known  $\text{CO}_2$  emission index (3160 g  $\text{CO}_2$  per kg fuel burnt) and  $\text{FSC} = 212$  mg/kg. In the FT the  $[\text{S}_{\text{T}}]_{\text{FT}}$  was about  $(1.5\text{--}3) \times 10^{12}$  cm<sup>-3</sup> (depending on the difference between the temperature at the sampling point and its value in the FT). Hence for an assumed  $\varepsilon \approx 2\%$  the total sulfur (VI) concentration at the sampling point would be of about sulfur (VI)<sub>P</sub>  $\approx 10^{12}$  cm<sup>-3</sup>. Neglecting wall losses in the FT (see below) would imply a mean value of sulfur

(VI)<sub>FT</sub> =  $4 \times 10^{10}$  cm<sup>-3</sup>. In comparison the mean total concentration of chemiions (CI) produced in the combustor is expected to be about  $[n_i]_{FT} \approx 6 \times 10^6$  cm<sup>-3</sup> (Arnold et al., 2002). Therefore, the CI formed in the combustor cannot deplete the sulfur (VI) gases through the ion–molecule reactions (1)–(9) in the FT. Thus only the interaction of sulfur molecules with reagent ions (i.e. NO<sub>3</sub><sup>-</sup>(HNO<sub>3</sub>)<sub>n</sub>) introduced into the FT may induce an observed their marked conversion to cluster ions.

Table 1 shows an example of the mass spectra of negative ions (in arbitrary units) obtained by the CIMS instrument. Case (a) corresponds to the jet engine not running and (b) the jet engine running at PS = 30% and burning fuel with FSC = 212 mg/kg. Spectrum (a) contains mostly the reagent ions NO<sub>3</sub><sup>-</sup>(HNO<sub>3</sub>)<sub>a</sub> with *a* equal to 0 (ion mass *m* = 62 of atomic units), 1 (*m* = 125), and 2 (*m* = 188). In addition hydrated forms of these ions are also noticeable (*m* = 80, 143, 161, 206). Spectrum (b) contains NO<sub>3</sub><sup>-</sup>(HNO<sub>3</sub>)<sub>a</sub> reagent ions but also product ions formed by ion–molecule reactions involving gaseous H<sub>2</sub>SO<sub>4</sub> and SO<sub>3</sub>: HSO<sub>4</sub><sup>-</sup> (*m* = 97), HSO<sub>4</sub><sup>-</sup>HNO<sub>3</sub> (*m* = 160), HSO<sub>4</sub><sup>-</sup>H<sub>2</sub>SO<sub>4</sub> (*m* = 195), SO<sub>4</sub><sup>-</sup>NO<sub>2</sub> (*m* = 142), HSO<sub>4</sub><sup>-</sup>SO<sub>3</sub> (*m* = 177) and possibly SO<sub>4</sub><sup>-</sup>(HNO<sub>3</sub>)NO<sub>2</sub> (*m* = 205). The ion identification is strongly supported also by jet fuel combustion measurements by our group using a quadrupole ion-trap mass spectrometer with a very high mass resolution and with an ion fragmentation mode of operation (Kiendler et al., 2000a). The presence of SO<sub>4</sub><sup>-</sup>NO<sub>2</sub> (*m* = 142), SO<sub>4</sub><sup>-</sup>(HNO<sub>3</sub>)NO<sub>2</sub> (*m* = 205) and

HSO<sub>4</sub><sup>-</sup>SO<sub>3</sub> (*m* = 177) indicates the presence of gaseous SO<sub>3</sub> in the FT. This suggests that a major fraction of SO<sub>3</sub> did not experience conversion to GSA in the free exhaust plume.

The measured ion abundance ratio *R*<sub>1</sub> of the sulfur-bearing ions (i.e. ions with HSO<sub>4</sub><sup>-</sup> and SO<sub>4</sub><sup>-</sup> cores) and all negative ions (i.e. with NO<sub>3</sub><sup>-</sup>, HSO<sub>4</sub><sup>-</sup> and SO<sub>4</sub><sup>-</sup> cores) ranges between 0.25 and 0.43. This ratio reflects the efficiency of the reagent ions conversion to sulfur-bearing negative ions and is approximately proportional to the gas-phase sulfur (VI) concentration. Its value is directly influenced by the conversion ( $\varepsilon$ ) of the fuel sulfur to gas-phase sulfur (VI). The measured abundance ratio *R*<sub>2</sub> of ion clusters containing SO<sub>4</sub><sup>-</sup> core ions and ion clusters containing both HSO<sub>4</sub><sup>-</sup> and SO<sub>4</sub><sup>-</sup> core ions ranges between 0.48 and 0.81. The core-ion SO<sub>4</sub><sup>-</sup> came from the neutral gas-phase SO<sub>3</sub>. Hence an appearance of such ion clusters indicates the incomplete conversion of SO<sub>3</sub> to H<sub>2</sub>SO<sub>4</sub> in the free exhaust plume and/or FT. So, if the amount of H<sub>2</sub>SO<sub>4</sub> formed from SO<sub>3</sub> directly in the FT (e.g. from the simulation) is known and we then compare the measured *R*<sub>2</sub> with the simulated *R*<sub>2</sub> ratio it is possible to define the initial concentrations of SO<sub>3</sub> and H<sub>2</sub>SO<sub>4</sub> at the sampling point in the exhaust.

The value of these ratios (*R*<sub>1</sub> and *R*<sub>2</sub>) were calculated using a detailed kinetic model (see below) of the evolution of sulfur gases and CI: (i) in the free exhaust plume (starting from the engine nozzle exit and up to the point of sampling); (ii) the ion-neutral gas phase composition transformation in the FT; and (iii) the exhaust gases interaction with reagent ions in the flow reactor (FR, i.e. the rest part of FT). The model takes into account the following processes: ion–ion recombination with respect to the ion mass growth via clustering, ion clustering due to interaction with H<sub>2</sub>O, SO<sub>3</sub>, H<sub>2</sub>SO<sub>4</sub> and HNO<sub>3</sub> gases, and gas-phase oxidation of SO<sub>3</sub> to H<sub>2</sub>SO<sub>4</sub>. Furthermore, the partial conversion of SO<sub>3</sub> to H<sub>2</sub>SO<sub>4</sub> taking place probably in the engine downstream of the combustor exit could be modeled.

### 3. Model

The measured *R*<sub>1</sub> and *R*<sub>2</sub> should be related to the concentrations of [SO<sub>3</sub>]<sub>FR</sub> and [H<sub>2</sub>SO<sub>4</sub>]<sub>FR</sub> of gaseous SO<sub>3</sub> and H<sub>2</sub>SO<sub>4</sub> in the flow reactor (FR) and FT. In turn these concentrations should be related to the concentrations [SO<sub>3</sub>]<sub>SP</sub> and [H<sub>2</sub>SO<sub>4</sub>]<sub>SP</sub> at the sampling point in the free exhaust plume of the engine. In order to determine [SO<sub>3</sub>]<sub>SP</sub> and [H<sub>2</sub>SO<sub>4</sub>]<sub>SP</sub> from the measured *R*<sub>1</sub> and *R*<sub>2</sub> a model calculation has been carried out considering several processes taking place in the FT and FR. These processes include: (a) SO<sub>3</sub> gas-phase conversion to H<sub>2</sub>SO<sub>4</sub>; (b) H<sub>2</sub>SO<sub>4</sub> loss at the inner walls of the FT and FR; (c) chemical evolution of the exhaust gases and

Table 1  
Mass spectra of negative ions (in arbitrary units) obtained by the CIMS instrument

Cluster ions	Mass (amu)	Relative abundance <sup>a</sup>	Relative abundance <sup>b</sup>
NO <sub>3</sub> <sup>-</sup>	62	7	5
NO <sub>3</sub> <sup>-</sup> (HNO <sub>3</sub> )	125	66	36
NO <sub>3</sub> <sup>-</sup> (HNO <sub>3</sub> ) <sub>2</sub>	188	94	50
NO <sub>3</sub> <sup>-</sup> (H <sub>2</sub> O)	80	0.7	0.5
NO <sub>3</sub> <sup>-</sup> (HNO <sub>3</sub> )(H <sub>2</sub> O)	143	12.5	
NO <sub>3</sub> <sup>-</sup> (HNO <sub>3</sub> )(H <sub>2</sub> O) <sub>2</sub>	161	4	
NO <sub>3</sub> <sup>-</sup> (HNO <sub>3</sub> ) <sub>2</sub> (H <sub>2</sub> O)	206	44	
HSO <sub>4</sub> <sup>-</sup>	97		2
HSO <sub>4</sub> <sup>-</sup> (HNO <sub>3</sub> )	160		19
SO <sub>4</sub> <sup>-</sup> (NO <sub>2</sub> )(H <sub>2</sub> O)			
HSO <sub>4</sub> <sup>-</sup> (H <sub>2</sub> SO <sub>4</sub> )	195		4
HSO <sub>4</sub> <sup>-</sup> (SO <sub>3</sub> )	177		7
HSO <sub>4</sub> <sup>-</sup> (H <sub>2</sub> O) <sub>2</sub>	133		0.5
SO <sub>4</sub> <sup>-</sup> (NO <sub>2</sub> )	142		16
SO <sub>4</sub> <sup>-</sup> (H <sub>2</sub> O)	114		0.2
SO <sub>4</sub> <sup>-</sup> (NO <sub>2</sub> )(HNO <sub>3</sub> )	205		21
SO <sub>4</sub> <sup>-</sup> (H <sub>2</sub> O) <sub>3</sub>	150		0.5

<sup>a</sup> Corresponds to the jet engine not running.

<sup>b</sup> The jet engine running at PS = 30% and burning fuel with FSC = 212 mg/kg.

CI and the reagent ions  $\text{NO}_3^-(\text{HNO}_3)_n$  introduced into the FR.

The reference model considers  $\varepsilon = ([\text{SO}_3] + [\text{H}_2\text{SO}_4]) / [\text{S}_T] = 0.02$  at the engine nozzle exit. This means that a production of sulfur (VI) has occurred in the engine and also may take place in the free exhaust plume up to the sampling point (at a distance of  $d = 1$  m). Two cases were considered with respect to the ratio  $\varepsilon_A = [\text{H}_2\text{SO}_4] / ([\text{SO}_3] + [\text{H}_2\text{SO}_4]) = [\text{H}_2\text{SO}_4] / (\varepsilon \cdot [\text{S}_T])$  at the engine nozzle exit: *case 1*:  $\varepsilon_A = 0.05$  and *case 2*:  $\varepsilon_A = 0.4$ . Another two cases were considered with regard to the “wall losses” of gas-phase  $\text{H}_2\text{SO}_4$  and  $\text{SO}_3$ : *case A*: no wall losses and *case B*: wall losses (determined by a radial diffusion of species to the wall) included in the model.

### 3.1. Chemistry model

Our model of the ion-neutral reactions consists of three packages: sulfur neutral chemistry, positive and negative ion clustering reactions and ion–ion recombination. We use a simplified version of the sulfur neutral chemistry. Since the model starts at the engine nozzle exit we consider  $\varepsilon$  and  $\varepsilon_A$  as input parameters which directly give us the initial concentration of  $\text{SO}_3$  and  $\text{H}_2\text{SO}_4$ . Also, since the sampling was done in the very hot exhaust at a short distance from the nozzle exit (1 m, i.e. in or near a hot potential jet core) and since the gases were then strongly diluted in the FT, it is appreciable to assume that there is no essential additional production of sulfur (VI) in the FT. Hence, only reactions describing the gas-phase chemical transformation of  $\text{SO}_3$  to  $\text{H}_2\text{SO}_4$  were considered. However, by contrast with a usually used model of the  $\text{H}_2\text{SO}_4$  formation in the aircraft gas-turbine engine exhaust (i.e. a one-step reaction  $\text{SO}_3 + \text{H}_2\text{O} \rightarrow \text{H}_2\text{SO}_4$  with a temperature-independent rate coefficient, e.g. Lukachko et al., 1998; Tremmel and Schumann, 1999; Starik et al., 2002) the considered mechanism includes as an intermediate step an association of  $\text{SO}_3$  and  $\text{H}_2\text{O}$  to form an adduct  $\text{SO}_3 \cdot \text{H}_2\text{O}$  which reacts with a second water molecule to produce  $\text{H}_2\text{SO}_4$  (Lovejoy et al., 1996; Jayne et al., 1997). It is important that this reaction has strong negative temperature dependence and is second order in the water concentration.

The main positive ion clusters in the experiment were exhaust positive CI formed in the combustor which most probably consisted of the hydronium ( $\text{H}_3\text{O}^+$ ) and/or hydrocarbon-oxygen core ions ( $\text{C}_x\text{H}_y\text{O}_z^+$ ) surrounded by water and hydrocarbon ligands (Fialkov, 1997; Kiendler and Arnold, 2002b; Sorokin and Arnold, submitted for publication). Positive ion clusters with the  $\text{NO}^+$  core-ion, which were modeled recently in Starik et al. (2002) were not considered in our model. In fact, such ion clusters were not detected in the exhaust of the real aircraft engine (Kiendler et al., 2000b; Kiendler and Arnold, 2002b). Moreover, numerous measurements of

the positive CI in burnt gases of hydrocarbon flames have shown (see review by Fialkov, 1997) that the formation of  $\text{NO}^+$  ions is seldom and takes place only in flames with a very high temperature in the reaction zone (e.g. as in pure oxygen flames like  $\text{C}_2\text{H}_2$  in  $\text{O}_2$ ). Thus, taking into account that the FT positive ion clusters mainly participate in the ion–ion recombination process, only the positive clusters  $\text{H}_3\text{O}^+(\text{H}_2\text{O})_n$  were considered in the model.

The main reagent ions in the experiment were  $\text{NO}_3^-(\text{HNO}_3)_{a=0,1,2}$ . The main clustering gases were  $\text{H}_2\text{O}$  ( $\text{CO}_2$  is another dominant combustion gas, but it was excluded from the model as less efficient in comparison with water),  $\text{HNO}_3$  (due to both a presence of this gas in jet engine exhaust and its possible production in the FR due to  $\text{HNO}_3$  ligand detachment from the reagent ion clusters),  $\text{SO}_3$  and  $\text{H}_2\text{SO}_4$  ( $\text{SO}_2$  was considered in the model as a non-clustering gas). Hydration of reagent and product ions by clustering to exhaust water vapor as expected do not disturb strongly the rate of reactions like (1)–(9) as was observed in Arnold et al. (1995) and Viggiano et al. (1997). The scheme of negative ion clusters reactions in combustion gases is very complicated (Fialkov, 1997). Additional to the (more or less) known nitrogen–sulfur anion chemistry it should also include the formation of negative hydrocarbon ions as was first detected in the exhaust of an aircraft gas-turbine engine by Kiendler et al. (2000a). However the kinetics of the negative “OHC-ions” formation is not known sufficiently to be included in our model. Since the dominant route of the considered ion–molecular processes is a conversion of the reagent ion clusters with an  $\text{NO}_3^-$  core ion to the product ion clusters with an  $\text{HSO}_4^-$  core ion the simplified version of the nitrogen–sulfur anion chemistry was used. The continuity equations in a box approach for 49 neutral and ion species were solved, including  $\text{H}_2\text{O}$ ,  $\text{SO}_3$ ,  $\text{H}_2\text{SO}_4$ ,  $\text{NO}_2$ ,  $\text{HNO}_3$  and  $\text{H}_3\text{O}^+(\text{H}_2\text{O})_{w=0-10}$ ,  $\text{NO}_3^-(\text{H}_2\text{O})_{w=0-2}$ ,  $\text{NO}_3^-(\text{HNO}_3)_{n=1,2}$ ,  $\text{NO}_3^-(\text{H}_2\text{O})(\text{HNO}_3)_2$ ,  $\text{HSO}_4^-(\text{H}_2\text{SO}_4)_{a=0-3}$ ,  $\text{HSO}_4^-(\text{HNO}_3)_{n=1,2}$ ,  $\text{HSO}_4^-(\text{H}_2\text{SO}_4)(\text{HNO}_3)(\text{H}_2\text{O})$ ,  $\text{HSO}_4^-(\text{H}_2\text{SO}_4)(\text{HNO}_3)$ ,  $\text{HSO}_4^-(\text{H}_2\text{O})(\text{HNO}_3)$ ,  $\text{HSO}_4^-(\text{H}_2\text{O})(\text{HNO}_3)_2$ ,  $\text{HSO}_4^-(\text{H}_2\text{SO}_4)(\text{H}_2\text{O})$ ,  $\text{HSO}_4^-(\text{H}_2\text{SO}_4)_2(\text{H}_2\text{O})$ ,  $\text{SO}_4^-(\text{SO}_3)_{m=0,1}$ ,  $\text{SO}_4^-(\text{H}_2\text{O})$ ,  $\text{SO}_4^-(\text{NO}_2)(\text{HNO}_3)_{n=0,1,2}$ ,  $\text{SO}_4^-(\text{NO}_2)(\text{H}_2\text{O})$ ,  $\text{SO}_4^-(\text{NO}_2)(\text{H}_2\text{O})(\text{HNO}_3)$ ,  $\text{SO}_4^-(\text{HNO}_3)$ ,  $(\text{SO}_3)_m=0,1$ ,  $\text{HSO}_4^-(\text{H}_2\text{SO}_4)_{a=0,1,2}(\text{SO}_3)$ ,  $\text{HSO}_4^-(\text{HNO}_3)$  ( $\text{SO}_3$ ). Forward rate coefficients for these reactions were taken from the available literature data. The NIST Database was used to calculate the reverse rate coefficients. A list of the ion cluster reaction data considered in the model can be obtained upon request.

### 3.2. Diffusion wall losses

In the flow tube, ions (ionic clusters and small charged aerosol particles, e.g. soot nuclei) and sulfur (VI) gases

may suffer “wall-losses” due to diffusion to the wall. When ions or charged particles (e.g. smallest soot particles) touch the wall, they are lost because of the neutralization of their charge. When neutral aerosol particles or neutral molecules touch the wall, they attach by van der Waals forces and are also lost.

The average flow velocity, determined using the total volumetric flow rate and the geometric cross section of the FT (4 cm i.d.) was about 28.7 m/s. The diffusion coefficient ( $D_g$ ) ranges between 0.17 and 0.12 cm<sup>2</sup>/s for “air” and SO<sub>3</sub> (H<sub>2</sub>SO<sub>4</sub>) molecules, respectively, at standard conditions. The Reynolds number for air flow in the FT (as a mean bulk) is about  $Re \approx 10^3$  for  $P_{FT} = 30$  hPa and  $T_{FT} = 330$ –350 K. Thus the flow is probably in the turbulent regime and mixing is achieved by eddy diffusion.

However, the solution of a system of even stationary diffusion equations for a chemically reactive turbulent flow in the cylindrical tube is too difficult. To simplify the study a first-order wall loss diffusion law was assumed. In this case for reacting with a wall of any component with concentration  $n_i$  the loss rate may be represented by  $(dn_i/dt)_{\text{loss}} \approx -k_w n_i$ , where  $k_w$  is a first-order diffusion loss rate coefficient. A unit probability of the reactive uptake coefficient per collision with the wall is assumed in this approach. The gas-phase diffusion-limited wall loss coefficient in a tubular flow reactor can be approximated by (Ferguson et al., 1969; Davies, 1973)

$$k_{wi} = \frac{3.66 D_g}{r^2 P_{FT}} \left( \frac{T_{FT}}{298} \right)^{1.89},$$

where  $D_g$  is the pressure-normalized (1 atm) gas-phase diffusion coefficient (varied for molecules and ion clusters),  $r$  is the tube inner radius ( $r = 2$  cm), and  $P_{FT}$ ,  $T_{FT}$  are the total pressure (30 hPa) and temperature (340 K) in the FT. This expression is derived when there is no saturation effect at the wall (i.e.  $n_i = 0$  at the wall). A value of  $D_g = 0.12$  cm<sup>2</sup>/s of the gas diffusion coefficient was taken for both SO<sub>3</sub> and H<sub>2</sub>SO<sub>4</sub> molecules (e.g. Jayne et al., 1997).

For ions and more massive ion clusters the respective ion diffusion coefficient depends on their electrical mobility ( $\mu$ ). The generally reported reduced mobility ( $\mu_0$ ) under standard conditions is related to  $\mu$  by:  $\mu = (\mu_0 / P_{FT})(T_{FT}/273)$ . The ion diffusion coefficient  $D_i$  and the mobility are related by (e.g. Mason and McDaniel, 1988):  $D_i = \mu k_B T / e$  where  $k_B$  is Boltzmann’s constant (in electric unit  $k_B = 8.615 \times 10^{-5}$  eV/K) and  $e$  is the elementary charge. The relationship between mobility and ion mass is somewhat uncertain. In our model we use a fit to experimental data to convert from atomic mass  $m_i$  in amu to mobility  $\mu_0$  in cm<sup>2</sup>/V/s from (Makela et al., 1996)

$$\mu_0 = \exp[-0.0347(\ln(m_i))^2 - 0.0376 \ln(m_i) + 1.4662].$$

The diffusion loss rates for ions and ion clusters were considered assuming they lose their charge when touching the wall. Note, the above diffusion-limited gas loss rate is typical for a laminar flow in the tube. The experiment was performed under a turbulent flow regime when diffusion losses may be essentially reduced in the laminar sub-layer near the wall (e.g. Jayne et al., 1997). So the comparison of results for cases A and B could elucidate the “wall-effect” in the interpretation of experimental data.

#### 4. Results and discussion

Fig. 1 shows for the cases 1A and 2A the variation with time (elapsed after sampling at the sampling point) of the gas-phase concentrations sulfur (VI), [SO<sub>3</sub>] and [H<sub>2</sub>SO<sub>4</sub>]. Generally sulfur (VI) remains nearly constant (no diffusion or any other losses) while [SO<sub>3</sub>] decreases and H<sub>2</sub>SO<sub>4</sub> increases (due to the gas-phase SO<sub>3</sub> conversion to H<sub>2</sub>SO<sub>4</sub>). For cases 1B and 2B (Fig. 2) sulfur (VI) decreases with time due to wall losses of gaseous SO<sub>3</sub> and H<sub>2</sub>SO<sub>4</sub>. Towards the end of the FT sulfur (VI) has decreased to approximately 50%. The decrease of [SO<sub>3</sub>] is even more pronounced than in case A due to additional wall losses. However [H<sub>2</sub>SO<sub>4</sub>] increases less steeply than in Fig. 1. In the case 2B it slightly decreases again towards the end of the FT reflecting the influence of wall losses. The gas-phase chemical production of sulfur (VI) cannot compensate the effect of wall losses. This run of the simulation was performed for  $T = 340$  K,  $\varepsilon = 2\%$  and a concentration of reagent ions of  $n_{R1} = 10^8$  cm<sup>-3</sup>. The variation of the concentration of reagent ions in the range  $10^7$ – $10^9$  cm<sup>-3</sup> has no essential effect on the concentrations of sulfur

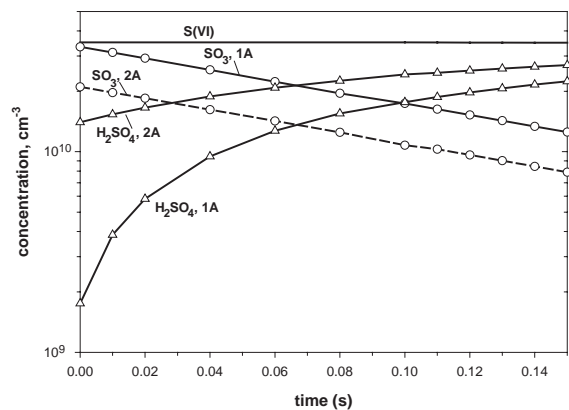


Fig. 1. Temporal evolution of gas-phase concentrations of sulfur (VI), [SO<sub>3</sub>] and [H<sub>2</sub>SO<sub>4</sub>] in the FR for cases 1A and 2A. Case 1:  $\varepsilon A = 0.05$ ; case 2:  $\varepsilon A = 0.4$ ; case A: no wall losses. For details see the text.

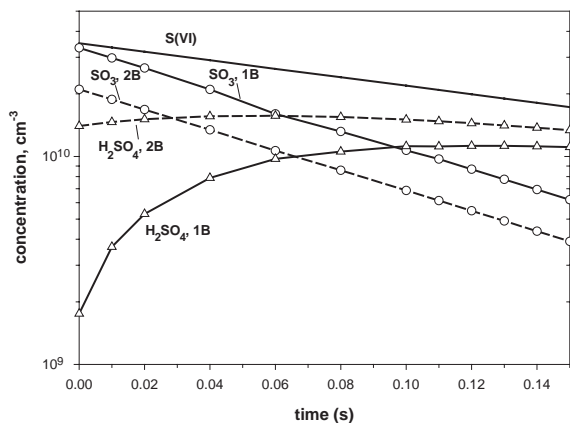


Fig. 2. Temporal evolution of gas-phase concentrations of sulfur (VI),  $[\text{SO}_3]$  and  $[\text{H}_2\text{SO}_4]$  in the FR for cases 1B and 2B. Case 1:  $\epsilon_A = 0.05$ ; case 2:  $\epsilon_A = 0.4$ ; case B: wall losses included in the model. For details see the text.

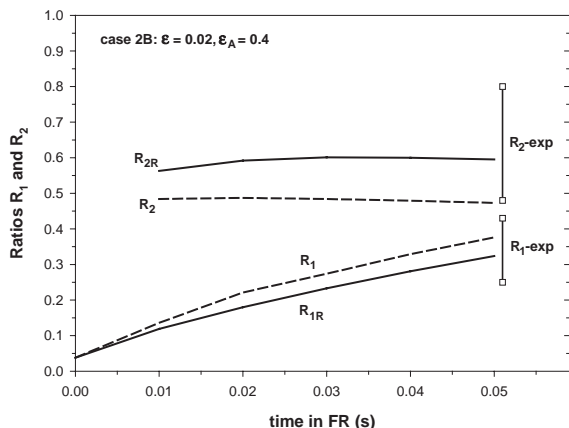


Fig. 3. The temporal evolution of the ion abundance ratios  $R_1$  and  $R_2$  for case 2B. Also given are the measured values. For details see the text.

(VI) gases. The experimental value of  $n_{\text{RI}}$  is expected in this range.

Fig. 3 shows for the case 2B the temporal evolution in the FR (elapsed from the time of reagent-ion introduction) of the ion abundance ratios  $R_1$  and  $R_2$  (dashed lines) and also the reduced abundance ratios  $R_{1\text{R}}$  and  $R_{2\text{R}}$  (thick lines) for ion clusters with masses smaller than 206 amu (this value corresponds to an upper mass limit of ions in the experiment). Also given in Fig. 3 are the measured values of  $R_1$  and  $R_2$ . Clearly the simulated reduced ratios compare more closely with the measured values in our work as they exclude the effect of ion mass growth outside the detected mass range. Both simulated ratios  $R_{1\text{R}}$  ( $R_1$ ) and  $R_{2\text{R}}$  ( $R_2$ ) increase with time. However, the increase of  $R_2$  and  $R_{2\text{R}}$  is very weak after

time  $t = 20$  ms. This reflects the achievement of an equilibrium distribution of negative sulfur-bearing cluster ions. The slope of the  $R_1$  and  $R_{1\text{R}}$  curves is approximately constant. The value of this slope of about  $4.5 \times 10^{-10} \text{ cm}^3/\text{s}$  is equal to an effective rate coefficient of a charge transfer reaction between reagent ions and sulfur (VI) molecules: sulfur (VI) +  $\text{NO}_3^- (\text{HNO}_3)_n \rightarrow [\text{product sulfur ions}] + \text{HNO}_3$ .

At the end of the FR both reduced ratios  $R_{1\text{R}}$  and  $R_{2\text{R}}$  are markedly different from the ratios  $R_1$  and  $R_2$ . This reflects the preferential growth of ions with  $\text{HSO}_4^- (\text{H}_2\text{SO}_4)_A$  where the A ligand is  $\text{H}_2\text{SO}_4$ ,  $\text{H}_2\text{O}$  or  $\text{HNO}_3$ . The reduced ratios  $R_{1\text{R}}$  and  $R_{2\text{R}}$  compare well with the experimental data. However, the ratio  $R_2$  is outside the experimental range. The simulation also shows that for the case 2A (no “wall losses”) the ratio  $R_{1\text{R}} = 0.48$  (2A case) is markedly above the experimental  $R_1$  range. Thus the next conclusions following Fig. 3 are: (i) Both “wall losses” and ion mass growth are important for the interpretation of measurement data. Up to 50% of ions may be lost on the walls of the flow tube (ii) For the basic case 2B the model value of  $R_{1\text{R}}$  and  $R_{2\text{R}}$  are in a good agreement with the experimental data.

Fig. 4 shows the simulated  $R_{1\text{R}}$  and  $R_{2\text{R}}$  versus the assumed  $\epsilon_A$  which indicates the relative abundance of  $\text{H}_2\text{SO}_4$  molecules in sulfur (VI) gases at the sampling point ( $\epsilon = 0.02$  and hereafter the index “R” for the reduced ratios  $R_{1\text{R}}$  and  $R_{2\text{R}}$  is omitted in the figures for simplicity). The variation of  $R_{2\text{R}}$  is more pronounced than that of  $R_{1\text{R}}$ . This reflects the influence of the charge-transfer reactions of the reagent ions with  $\text{SO}_3$  and  $\text{H}_2\text{SO}_4$ . The more  $\text{H}_2\text{SO}_4$  (formed in reaction  $\text{SO}_3 + \text{H}_2\text{O}$ ) is present, the less becomes the value of  $R_2$ .

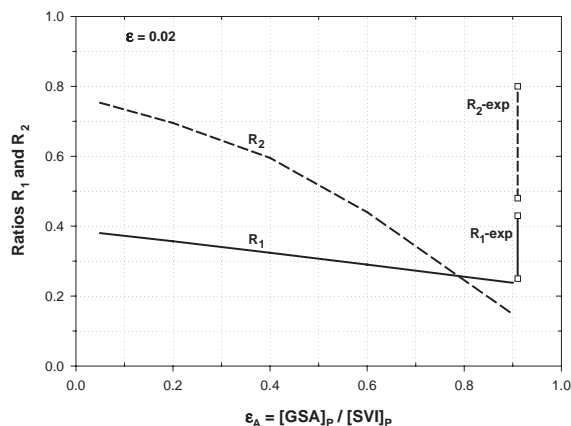


Fig. 4. Comparison of model ratios  $R_1$  and  $R_2$  with experimental data versus the assumed relative abundance  $\epsilon_A$  of  $\text{H}_2\text{SO}_4$  molecules in sulfur (VI) gases at the sampling point. For details see the text.

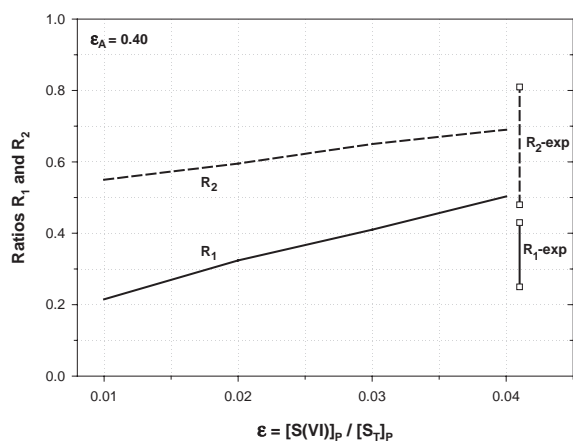


Fig. 5. Comparison of model ratios  $R_1$  and  $R_2$  with experimental data versus the assumed  $\varepsilon$  (fuel sulfur conversion factor) at the sampling point. For details see the text.

Fig. 4 also shows that model ratios compare with the experimental data for  $\varepsilon_A \leq 0.5$ . This means that at least 50% of sulfur (VI) gases at the sampling point should be  $\text{SO}_3$  to compare with the experimental data. Interestingly, even for  $\varepsilon_A = 0$  (no sulfuric acid in the exhaust, i.e. sulfur (VI) =  $\text{SO}_3$ ) the time the exhaust spent in the FT is sufficient for the formation of gaseous  $\text{H}_2\text{SO}_4$  comparable with the experimental data. Hence it seems that at the sampling point  $\text{SO}_3$  represents a major fraction of sulfur (VI) and substantial  $\text{SO}_3$  conversion to  $\text{H}_2\text{SO}_4$  took place in the sampling line and the FR.

Fig. 5 shows the simulated  $R_{1R}$  and  $R_{2R}$  versus the assumed  $\varepsilon$  ( $\varepsilon_A = 0.4$ ). Also given for comparison are the measured ratios. The comparison suggests that the experimental  $R_1$  and  $R_2$  are consistent with  $\varepsilon_P = 2.3 \pm 1\%$  (the value of a fuel sulfur conversion factor  $\varepsilon$  at the sampling point in exhaust). When compared with previous  $\varepsilon$  reported in the literature ( $\varepsilon < 5.1\%$ , see above) our present value  $\varepsilon_P = 2.3 \pm 1\%$  is near to the lower side. However when compared with reported value of  $\varepsilon$  which were previously obtained by measuring gaseous sulfur (VI) (all made by our group with CIMS) the present value is in reasonably good agreement.

## 5. Conclusions

The major results of the presented CIMS experiments made in the exhaust of an aircraft gas-turbine combustor and their interpretation with a model simulation are: (i) In the exhaust plume both  $\text{SO}_3$  and  $\text{H}_2\text{SO}_4$  are present; (ii) The sulfur (VI) abundance ratio  $\varepsilon$  is in  $2.3 \pm 1\%$  at an exhaust age of about 5 ms from the combustor exit; (iii) The  $\text{SO}_3$  molecules represent a

major fraction of sulfur (VI) in the exhaust behind the combustor and an essential  $\text{SO}_3$  conversion to  $\text{H}_2\text{SO}_4$  takes place in the sampling line where the exhaust gases spend a sufficiently long time and where the temperature is markedly lower than in the hot exhaust.

From (i) and (iii) it can be concluded that  $\text{SO}_3$  conversion to  $\text{H}_2\text{SO}_4$  is most probably not completed in the engine where the temperature is too high and even not at a plume age of 75 ms (about 15 m downstream of the engine exit plane). However  $\text{SO}_3$  conversion to  $\text{H}_2\text{SO}_4$  will be rapidly completed due to the low plume temperature.

From (ii) it can be concluded that the major fraction of sulfur (VI) gases forms in the aircraft combustor and that their formation is inefficient in the exhaust plume and in the post-combustor flow inside the aircraft engine. The coincidence of  $\varepsilon$  from our work (measurements with the sampling point in the exhaust just behind the combustor exit) and  $\varepsilon$  from measurements in an exhaust plume at a plume age of about 1 s strongly supports this conclusion.

## Acknowledgements

This project was funded by DLR (SULFUR campaign), Max-Planck-Society, and partially by the INTAS project OPEN 2000-460

## References

- Arnold, S.T., Morris, R.A., Viggiano, A.A., Jayne, J.T., 1995. Ion chemistry relevant for chemical ionization detection of  $\text{SO}_3$ . *Journal of Geophysical Research* 100, 14141–14146.
- Arnold, F., Wohlfrom, K.H., Klemm, M.W., Schneider, J., Gollinger, K., Schumann, U., Busen, R., 1998. First gaseous ion composition measurements in the exhaust plume of a jet aircraft in flight: implication for gaseous sulfuric acid, aerosols, and chemions. *Geophysical Research Letters* 25, 2137–2140.
- Arnold, F., Kiendler, A., Wiedemer, V., Aberle, S., Stimp, T., Busen, R., 2002. Chemion concentration measurements in jet engine exhaust at the ground: implications for ion chemistry and aerosol formation in the wake of a jet aircraft. *Geophysical Research Letters* 27, 1723–1726.
- Curtius, J., Sierau, B., Arnold, F., Baumann, R., Busen, R., Schulte, P., Schumann, U., 1998. First direct sulfuric acid detection in the exhaust plume of a jet aircraft in flight. *Geophysical Research Letters* 25, 923–926.
- Curtius, J., Arnold, F., Schulte, P., 2002. Sulfuric acid measurements in the exhaust plume of a jet aircraft in flight: implications for the sulfuric acid formation efficiency. *Geophysical Research Letters* 29, 17.1–17.4.
- Davies, C.N., 1973. Diffusion and sedimentation of aerosol particles from poiseuille flow in pipes. *Journal of Aerosol Science* 4, 317.

- Ferguson, E.E., Fehsenfeld, F.C., Schmeltekopl, A.L., 1969. Advance in atom and molecule Physics 5, 1.
- Fialkov, A.B., 1997. Investigation on ions in flames. Progress in Energy and Combustion Science 23, 399–528.
- Frenzel, A., Arnold, F., 1994. Sulfuric acid cluster ion formation by jet engines: implications for sulfuric acid formation and nucleation. DLR-Mitt. 94-06, Deutsches Zentrum für Luft-und Raumfahrt, Köln, Germany, pp. 106–112.
- IPCC (Intergovernmental Panel of Climate Change), 1999. In: Penner, J., Lister, D., Griggs, D., Dokken, D., McFarland, M. (Eds.), Aviation and the Global Atmosphere. Cambridge University Press, Cambridge, UK.
- Jayne, J.T., Pöschl, U., Chen, Yu, Dai, D., Molina, L.T., Worsnop, D.R., Kolb, C.E., Molina, M.J., 1997. Pressure and temperature dependence of the gas-phase reaction of SO<sub>3</sub> with H<sub>2</sub>O and the heterogeneous reaction of SO<sub>3</sub> with H<sub>2</sub>O/H<sub>2</sub>SO<sub>4</sub> surfaces. Journal of Physical Chemistry A101, 10000–10011.
- Karcher, B., 1996. Aircraft-generated aerosols and visible contrails. Geophysical Research Letters 23, 1933–1936.
- Karcher, B., 1998. On the potential importance of sulfur-induced activation of soot particles in nascent aircraft exhaust plumes. Atmospheric Research 46, 293–305.
- Katragkou, E., Wilhelm, S., Arnold, F., Wilson, C., 2003. First gaseous Sulfur (VI) measurements in the simulated internal flow of an aircraft gas turbine engine during project PartEmiss. Geophysical Research Letters, accepted.
- Kiendler, A., Arnold, F., 2002a. Unambiguous identification and measurement of sulphuric acid cluster chemions in aircraft jet engine exhaust. Atmospheric Environment 36, 1757–1761.
- Kiendler, A., Arnold, F., 2002b. First composition measurements of positive chemions in aircraft jet engine exhaust: detection of numerous ion species containing organic compounds. Atmospheric Environment 36, 2979–2984.
- Kiendler, A., Aberle, S., Arnold, F., 2000a. Negative chemions formed in jet fuel combustion: new insights from jet engine and laboratory measurements using a novel quadrupole ion trap mass spectrometer apparatus. Atmospheric Environment 34, 2623–2632.
- Kiendler, A., Aberle, S., Arnold, F., 2000b. Positive ion chemistry in the exhaust plumes of an aircraft engine and a burner: investigations with a quadrupole ion trap mass spectrometer. Atmospheric Environment 34, 4787–4793.
- Lovejoy, E.R., Hanson, D.R., Huey, L.G., 1996. Kinetics and products of the gas-phase reaction of SO<sub>3</sub> with water. Journal of Physical Chemistry 100, 19911–19916.
- Lukachko, S.P., Waitz, I.A., Miake-Lye, R.C., Brown, R.C., Anderson, M.R., 1998. Production of sulphate aerosol precursors in the turbine and exhaust nozzle of an aircraft engine. Journal of Geophysical Research 103, 16159–16174.
- Makelae, J.M., Jokinen, V., Mattila, T., Ukkonen, A., Keskinen, J., 1996. Mobility distribution of acetone cluster ions. Journal of Aerosol Science 27, 175–190.
- Mason, E.A., McDaniel, E.W., 1988. Transport Properties of Ions in Gases. Wiley, New York.
- Reiner, T., Arnold, F., 1993. Laboratory flow reactor measurements of the reaction SO<sub>3</sub> + H<sub>2</sub>O + M → H<sub>2</sub>SO<sub>4</sub> + M: implications for gaseous H<sub>2</sub>SO<sub>4</sub> and aerosol formation. Geophysical Research Letters 20, 2659–2662.
- Schumann, U., Arnold, F., Busen, R., Curties, J., Kärcher, B., Kiendler, A., Petzold, A., Schlager, H., Schroder, F., Wohlfrom, K.-H., 2002. Influence of fuel sulfur on the composition of aircraft exhaust plumes: the experiments SULFUR 1-7. Journal of Geophysical Research 107, 10.1029/2001JD000813.
- Sorokin, A., Arnold, F. Electrically charged small soot particles in the exhaust of an aircraft gas turbine engine combustor: comparison of model and experiment. Atmospheric Environment, submitted for publication.
- Starik, A.M., Savel'ev, A.M., Titova, N.S., Schumann, U., 2002. Modeling of sulfur gases and chemions in aircraft engines. Aerospace Science and Technology 6, 63–81.
- Su, T., Chesnavich, W.J., 1982. Parameterization of the ion-polar molecule rate constant by trajectory calculations. Journal of Chemical Physics 76, 5183–5185.
- Tremmel, H.G., Schumann, U., 1999. Model simulations of fuel sulfur conversion efficiencies in an aircraft engine: dependence on reaction rate constants and initial species mixing ratios. Aerospace Science and Technology 3 (7), 417–430.
- Viggiano, A.A., Seeley, J.V., Mundis, P.L., Williamson, J.S., Morris, R.A., 1997. Rate constants for the reactions of XO<sub>3</sub><sup>-</sup>(H<sub>2</sub>O)<sub>n</sub> (X=C, HC, and N) and NO<sub>3</sub><sup>-</sup>(HNO<sub>3</sub>)<sub>n</sub> with H<sub>2</sub>SO<sub>4</sub>: implications for atmospheric detection of H<sub>2</sub>SO<sub>4</sub>. Journal of Physical Chemistry A101, 8275–8278.
- Yu, F., Turco, R.P., 1997. The role of ions in the formation and evolution of particles in aircraft plumes. Geophysical Research Letters 24, 1927–1930.
- Zhao, J., Turco, R.P., 1995. Nucleation simulation in the wake of a jet aircraft in stratospheric flight. Journal of Aerosol Science 26, 779–795.